14. Coherence Flow Networks

A popular approach to the description of NMR pulse sequences comes from a simple vector model[1,2] in which the motion of the spins subjected to RF pulses and chemical shifts is described by the rotations of a classical vector in three-dimensional space. The major weakness in this model is that spin systems that contain scalar coupling are not adequately described. The ultimate description of NMR experiments is through the application of density matrix theory. This approach, while extremely powerful, is often difficult to the uninitiated. In 1983, several groups independently introduced the product operator formalism as a simplification of density matrix theory.[3,4,5] In this treatment, the density matrix is expanded as a linear combination of a basis set of operators. The product operators resolve the density matrix into a set of elements that can be visualized as generalized magnetization vectors, referred to as coherences. The motion of the product operators subjected to RF pulses, chemical shifts, and coupling is analogous to the motion of the classical magnetization vectors in three-dimensional space and thus the popular vector model can be extended to spin systems that contain scalar coupling.

Currently, the majority of experiments in the literature are described by using one or another implementation of the product operator formalism. Product operators, while very convenient for a simple description of NMR experiments, are not very compact for complex calculations. A given pulse sequence can generate many product operator terms that are multiplied by various cosine and sine coefficients. Many of these terms are not physically observable or are eliminated by phase cycling routines, so the description of pulse sequences with product operators is commonly abbreviated by retaining only the relevant terms. Usually, only a few of the important coherences are described at various points in the pulse sequence to give a sense of the flow of coherence from one section of the experiment to the next. Much of the detail of the mechanism of coherence transfer and modulation is removed, leaving behind the essentials of the pulse sequence. Eggenberger and Bodenhausen[6] have used a graphical approach to simplify the product operator notation. Their description (EB) does not compromise the rigor of the product operator treatment and allows for the exact description of experiments. While EB is a useful simplification for the practicing NMR spectroscopist, it lacks an overview quality that can be useful in a "top-down" approach to NMR spectroscopy.

Introduced here is a systematic, graphical description of multipulse experiments in terms of the flow of coherence during a pulse sequence. Coherence flow network (CFN) diagrams can be used to accurately describe the mechanisms of coherence transfer and modulation used in multipulsed NMR experiments. Experiments can be written at a very qualitative level for "back-of-the-envelope" discussions or, with increasing detail, at a level that is equivalent to the product operator formalism. The "top-down" approach of CFN is a very natural procedure for the solution of problems

involving NMR spectroscopy.

14.1. Description of the Coherence Flow Network.

A coherence flow network (CFN) describes the flow of coherence during an NMR pulse sequence. The flow of coherence is the pathway followed by the signal of interest that is selected by the pulse sequence and its associated phase cycle. The CFN description does not detail the pulse sequence nor the phase cycle that is used to accumulate the experimental data, but the essence of the product operator description is abstracted into a visual form.

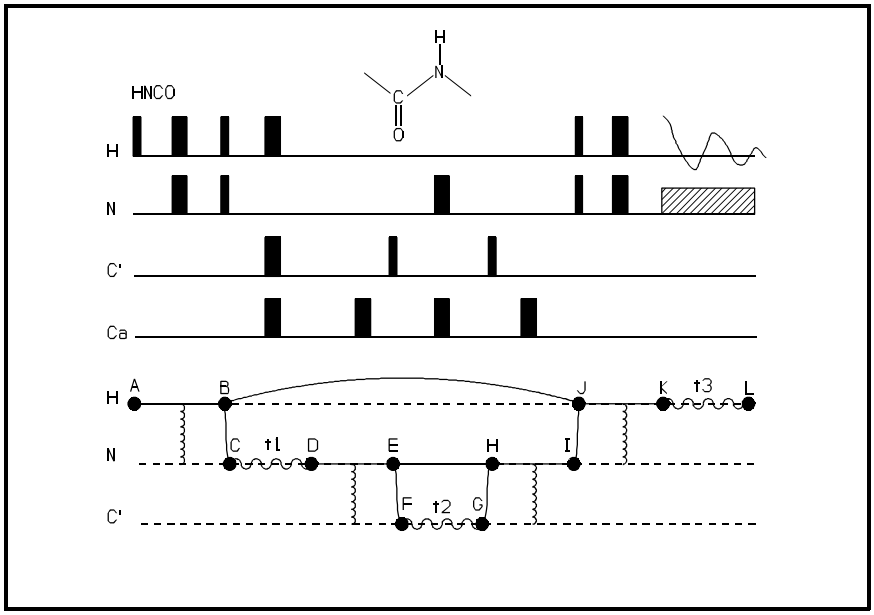

Figure 14.1. Pulse Sequence and CFN for the three dimensional HNCO experiment.

As an introduction to the uses of a CFN in the understanding of a complicated pulse sequence, the *three-dimensional* HNCO experiment[7] is shown in Figure 14.1. The spectrum obtained from this sequence correlates the chemical shifts of the amide ^{1}H, the amide ^{15}N, and the attached carbonyl ^{13}C. At the top of the figure is the pulse sequence that might be presented in a paper discussing this experiment. In such a paper[8], one might read ". . . magnetization originating from NH protons is transferred to the directly bonded ^{15}N spins using an INEPT sequence, following which ^{15}N magnetization evolves exclusively under the influence of the ^{15}N chemical shift because of ^{1}H, ^{13}CO and $^{13}C^{\alpha}$ decoupling through the application of 180° pulses at the midpoint of the t_1 interval . . . " The text continues to describe what happens next in the sequence continuing through the detection of the NH protons. This description is a detailed visualization of the experiment without any physical "picture" being drawn. At the bottom of Figure 14.1 is the CFN of this experiment. The verbal description of the CFN is very similar to that above, but the advantage of the CFN to the reader is that no "minds eye" view of the coherence flow is necessary. The CFN is an attempt to graphically represent the verbal description accompanying a pulse sequence.

Each observed signal in a multipulsed NMR experiment can be systematically traced from a *source* of magnetization by *evolution* of coherence through intervening *states* to a final *sink* corresponding to the detection of the observed resonance. The evolution of coherence through the states represents the motion of the spin system under the influence of the Hamiltonian operators that are active during various evolution periods of the pulse sequence. By following the evolution of the spin coherence through the pulse sequence, the point-of-origin of information, such as the evolution period for indirectly detected nuclei and coherence transfer steps, is easily localized to a particular part of an experiment.
In a coherence flow network, the evolution of a coherence is assigned a primitive, graphical operator (*flow primitive*) between every pair of states that are visited by the coherence flow. Flow primitives have associated *modifiers* that detail the nature of interactions of the spin assigned to the flow primitive with other spins in the system. Flow primitives and modifiers are further combined systematically to construct a coherence flow network.

Table 14.1 contains descriptions of the primitive operators that are used in creating CFN diagrams. Every spin that is involved in the coherence flow is assigned a *tier* that is designated by a horizontal dashed line. On each spin tier, various CFN primitives are used to describe the evolution of the spin between states. States, designated by circles, are found at the junction of two adjacent evolutions. In an experiment with many different source spins, the coherence flow networks of the various spins overlap, possibly with multiple networks having a common sink. Similarly, diagrams with a single source spin that split into several paths having different sinks represent overlapping networks. However, for a given, observed coherence there is only one source and one sink.

If a spin is not involved in a coherence, i.e., the spin is at Boltzmann equilibrium or saturated, or if a coherence does not contribute to the final signal then there is no CFN flow primitive or modifier drawn on that spin tier during that period of the pulse sequence. CFN primitives that connect two states located on the same tier represent evolutions involving either transverse magnetization (*e.g.,* $\mathbf{I_x}$), the Z component of an antiphase coherence (*e.g.,* $\mathbf{2I_zS_x}$), or a longitudinal spin order state (*e.g.,* $\mathbf{2I_zS_z}$) for the spin on that tier. Flow primitives drawn as either straight lines (Table 14.1 **E**) or wavy lines between states (Table 14.1 CS) represent inphase, transverse magnetization while a curved arc represents the Z state of an antiphase coherence (Table 14.1 **Z**). Flow primitives can have added modifiers that connect two different spin tiers. These primitives are vertical wavy lines representing "active" coupling (Table 14.1 **A**) or hashed boxes representing "passive" coupling (Table 14.1 **P**) Active coupling causes the initial state to oscillate between inphase and antiphase states. If the initial state was inphase, then the final state is an antiphase state (with a coefficient of $\sin(\pi J_{IS}t)$). Likewise, if the initial state was antiphase, then the final state is inphase. A passive coupling modulates an initial state by $\cos(\pi J_{IS}t)$ but does not allow for the conversion

between inphase and antiphase states. Couplings between more than one spin pair are designated by multiple **A** or **P** modifiers emanating from a single flow primitive.

CFN flow primitives connecting states on different tiers represent the transfer of coherence from one spin to another (Table 14.1 **CT**). These transfers usually pass through an antiphase state formed from the spin states involved in the coherence transfer. The **CT** primitive is represented by a solid line connecting the two states that are involved. Transfer by an isotropic mixing sequence (as in TOCSY or HOHAHA experiments) is represented by multiple **CT** primitives connecting one state to all other states that are involved in the isotropic mixing and then enclosed in a box (Table 14.1 **T**).

A CFN for an experiment is created by the combination of flow primitives, modifiers, and states. One begins by generating a tier for every spin that is involved in the coherence flow. The source and sink are chosen. Then flow primitives and modifiers are introduced to emulate the coherence flow between states during the pulse sequence. The CFN, which is generated, represents the overall flow of coherence *after all phase cycling and pulsed field gradient coherence selection*.

14.2. Composite Rotations

The CFN representation is closely related to concept of composite rotations,[1] in which several rotation operators are combined into one or a few simple rotations. Composite rotations can be used as 'black boxes' for the description of common segments of pulse sequences. The evolution of coherence between states during a segment of a pulse sequence is dictated by the effective Hamiltonian operator that governs evolution during that segment. The effective Hamiltonian can consist of any combination of operators, such as, chemical shift operators, scalar coupling operators, dipolar operators, and radiofrequency fields. The evolution of the spin system under a given effective Hamiltonian operator can be written as the product of all of the unitary operators that represent the individual parts of the Hamiltonian.

Table 14.1 Coherence Flow Network Primitives

	Operator	Effect	Example
CS		Transverse magnetization with chemical shift precession.	$\mathbf{I}_x$ $=\omega_I t\hat{\mathbf{I}}_z=>$ $\mathbf{I}_x \cos(\omega_I t) + \mathbf{I}_y \sin(\omega_I t)$
TC		Transverse magnetization with constant time chemical shift precession.	$\mathbf{I}_x$ $=\omega_I(T-t/2)\hat{\mathbf{I}}_z=>$ $=\pi\hat{\mathbf{I}}_x=>$ $=\omega_I(T+t/2)\hat{\mathbf{I}}_z=>$ $\mathbf{I}_x \cos(\omega_I t) + \mathbf{I}_y\sin(\omega_I t)$
E		Transverse magnetization without chemical shift precession.	$\mathbf{I}_y$ $=\omega_I t\hat{\mathbf{I}}_z=>$ $=\pi\hat{\mathbf{I}}_x=>$ $=\omega_I t\hat{\mathbf{I}}_z=>$ $-\mathbf{I}_y$
Z		Evolution with retention of antiphase state.	$\mathbf{2}\ \underline{\mathbf{I}_z}\ \mathbf{S}_x$ $=\pi/2\ \mathbf{2}\hat{\mathbf{S}}_z\mathbf{T}_z=>$ $\mathbf{4}\ \underline{\mathbf{I}_z}\ \mathbf{S}_y\mathbf{T}_z$
CT	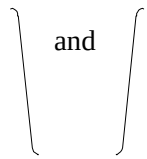	Coherence transfer (between spins).	$\mathbf{2I}_y\mathbf{S}_z$ $=\pi/2(\hat{\mathbf{I}}_x+\hat{\mathbf{S}}_x)=>$ $-\mathbf{2I}_z\mathbf{S}_y$

Table 14.1 Coherence Flow Network Primitives

	Operator	Effect	Example
T	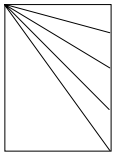	Isotropic mixing	TOCSY, HOHAHA
N		Incoherent transfer by longitudinal cross-relaxation.	NOESY, Chemical Exchange
R		Incoherent transfer by transverse cross-relaxation.	ROESY, Chemical Exchange
A		Active coupling, oscillation between inphase and antiphase states.	$\mathbf{I}_x$ $=\pi J_{IS}\mathbf{t}\ 2\hat{\mathbf{I}}_z\hat{\mathbf{S}}_z \Rightarrow$ $\mathbf{2I}_y\mathbf{S}_z \sin(\pi J_{IS}\mathbf{t})$
P		Passive coupling, no oscillation between inphase and antiphase states.	$\mathbf{I}_x$ $=\pi J_{IS}\mathbf{t}2\hat{\mathbf{I}}_z\hat{\mathbf{S}}_z \Rightarrow$ $\mathbf{I}_x \cos(\pi J_{IS}t)$

Table 14.1 Coherence Flow Network Primitives

	Operator	Effect	Example
CC		Antiphase buildup due to cross correlation	$\mathbf{I_x}$ $=\Gamma_{IS}*t=>$ $a*\mathbf{2I_xS_z}$
T1		Longitudinal relaxation, T_1	Inversion-recovery
T1R		Rotating frame longitudinal relaxation, $T_{1\rho}$	Spin-lock
T2		Transverse relaxation, T_2	Spin-echo

A series of **i** rotations $\mathbf{U}_i$ representing the various Hamiltonian operators during the pulse sequence can be written as:

$$\sigma_0 = \mathbf{U_1} => = \mathbf{U_2} => = \mathbf{U_3} => = \mathbf{U_4} => \ldots = \mathbf{U_i} => \sigma_t \qquad (14.2.1)$$

These distinct rotations can always be combined into a single total rotation applied to σ_0.

$$\sigma_0 = \mathbf{U_{total}} => \sigma_t \qquad (14.2.2)$$

Usually, $\mathbf{U_{total}}$ is a simple rotation or at most a short series of a few simple rotations. By reducing the pulse sequence to a series of simple propagators, the experimental method can be described in a simple and straightforward manner.

14.3. Spin Echo Sequence for an Isolated Spin

A spin echo sequence (τ - 180_ϕ - τ) refocuses the chemical shift (and any dephasing due to field inhomogeneity) of a transverse isolated spin, creating an effective Hamiltonian operator that does not contain a chemical shift operator. This sequence does not alter the state of the spin system except for a phase shift.

The pulse sequence for the spin echo sequence with an initial 90° pulse applied to a single isolated spin **I** is given in Equation 14.3.1.

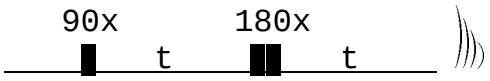

(14.3.1)

The product operator description for this sequence follows (Equation 14.3.2).

$$\mathbf{I_z} = \pi/2\hat{\mathbf{I}}_x => -\mathbf{I_y} = \omega_I t\hat{\mathbf{I}}_z => -\mathbf{I_y}\cos\omega_I t + \mathbf{I_x}\sin\omega_I t$$

$$= \pi\hat{\mathbf{I}}_x => \mathbf{I_y}\cos\omega_I t + \mathbf{I_x}\sin\omega_I t$$

$$= \omega_I t\hat{\mathbf{I}}_z => (\mathbf{I_y}\cos\omega_I t - \mathbf{I_x}\sin\omega_I t)\cos\omega_I t$$

$$+ (\mathbf{I_x}\cos\omega_I t + \mathbf{I_y}\sin\omega_I t)\sin\omega_I t$$

$$\equiv \mathbf{I_y}(\cos^2\omega_I t + \sin^2\omega_I t)$$

$$\equiv \mathbf{I_y} \qquad (14.3.2)$$

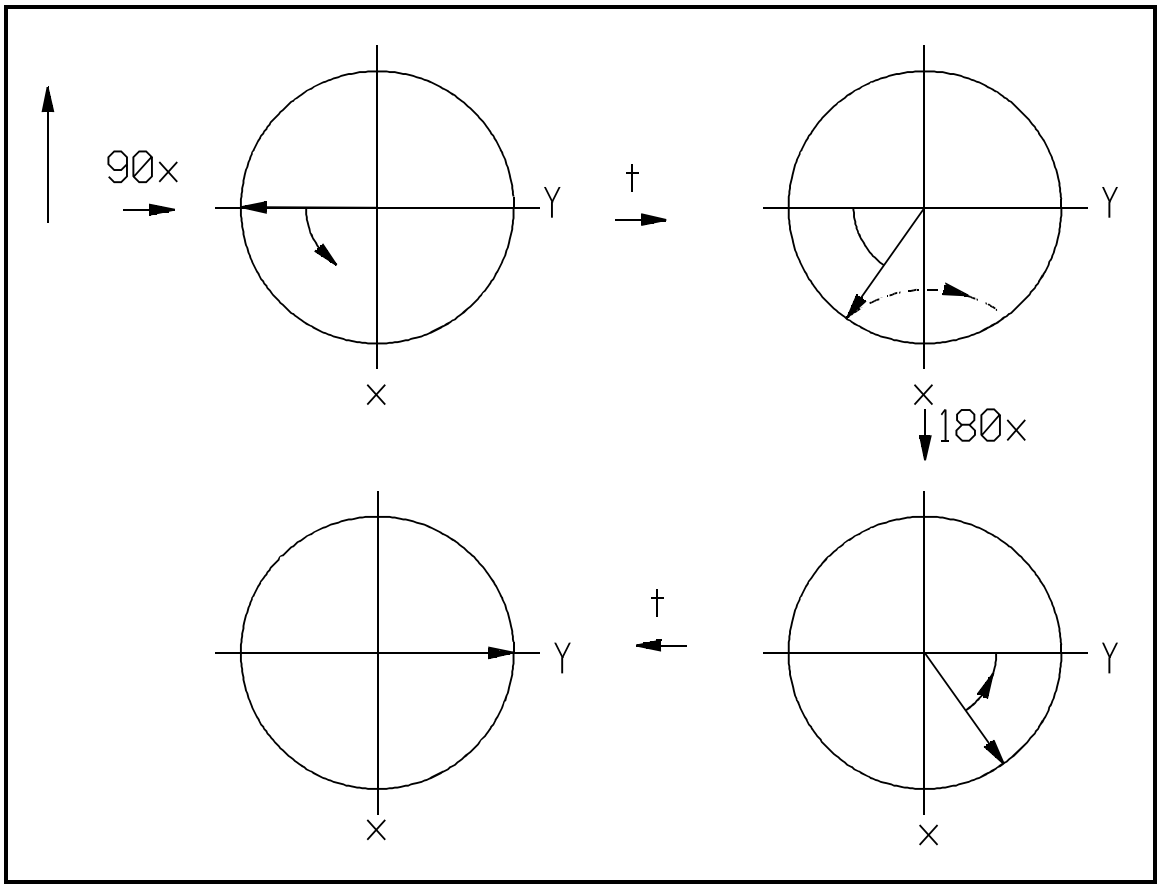

Figure 14.2. Vector picture of spin echo sequence for an isolated spin.

The sequence of the rotation operators is given in Equation 14.3.3

$$=\omega_I t\hat{I}_z=> \ =\pi\hat{I}_\phi=> \ =\omega_I t\hat{I}_z=> \qquad (14.3.3)$$

representing a free evolution under the chemical shift operator ($\hat{I}_z$), a 180° pulse about a ϕ axis, and finally, a second free evolution due to chemical shift. This sequence can be simplified by introducing the unit operator (Equation 14.3.4).

$$=\pi\hat{I}_\phi=> \ =-\pi\hat{I}_\phi=> \qquad (14.3.4)$$

at the beginning of Equation 14.3.3.

$$=\pi\hat{I}_\phi=> \{ =-\pi\hat{I}_\phi=> =\omega_I t\hat{I}_z=> =\pi\hat{I}_\phi=> \} =\omega_I t\hat{I}_z=>. \qquad (14.3.5)$$

The portion of Equation 14.3.5 isolated by brackets can be simplified by use of the equivalent rotation[3]

$=-\pi\hat{\mathbf{I}}_{\phi}=> =\omega_I t\hat{\mathbf{I}}_z=> =\pi\hat{\mathbf{I}}_{\phi}=> \quad = \quad =-\omega_I t\hat{\mathbf{I}}_z=>.$ (14.3.6)

This and similar equivalent rotations are simple to remember:

> *If there are two identical operators with opposite signs surrounding another operator, then the equivalent rotation is obtained by the rotation of the central operator by the third operator. This does not always give simple results, but with judicious choices of the inserted unit operators, the sequence can be often simplified.*

Upon substitution of the equivalent rotation into Eqution 14.3.5, the sequence becomes Equation 14.3.7.

$=\pi\hat{\mathbf{I}}_{\phi}=> =-\omega_I t\hat{\mathbf{I}}_z=> =\omega_I t\hat{\mathbf{I}}_z=>$ (14.3.7)

The adjacent, inverse rotations $=-\omega_I t\hat{\mathbf{I}}_z=>$ and $=\omega_I t\hat{\mathbf{I}}_z=>$ are equivalent to the identity operator $=\hat{\mathbf{I}}_E=>$, which does not rotate the spin. The sequence can then be further simplified to Equation 14.3.8.

$=\pi\hat{\mathbf{I}}_{\phi}=>$ (14.3.8)

The final phase of the spin depends on the phase of the 180° pulse, but no chemical shift evolution occurs. This is also formally equivalent to the refocusing of spin isochromats in an inhomogeneous magnetic field where the chemical shift operator is replaced by a spatially-varying magnetic field strength.

In CFN notation this spin echo sequence is represented by a primitive that is diagrammed as a straight line (Table 14.1 **E**), signifying that no chemical shift evolution occurs between the two states that are connected by the spin echo sequence. The phase of the coherence is not explicitly represented in the CFN description. The phase information, however, is implicitly held in each individual state. By explicitly describing the states, CFN becomes equivalent to the product operator formalism.

Table 14.2. Several important CFN diagrams

CFN diagram	Pulse sequence	Composite rotation
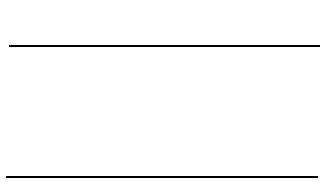 A	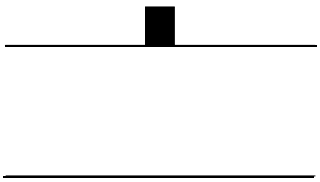	$=\pi\hat{I}_{\phi}=>$
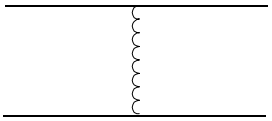 B	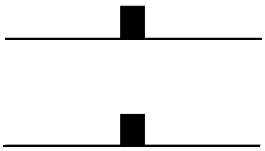	$=\pi\hat{I}_{\phi}=>$ $=\pi J_{IS}t2\hat{I}_z\hat{S}_z=>$
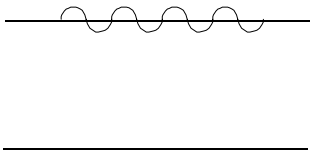 C	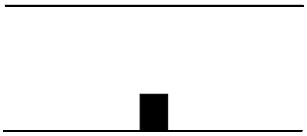	$=\omega_I t\hat{I}_z=>$
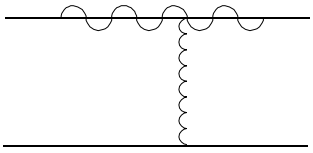 D		$=\omega_I t\hat{I}_z=>$ $=\pi J_{IS}t2\hat{I}_z\hat{S}_z=>$

14.4. Coupled Two-Spin System - Selective I 180° pulse

Four important evolutions for coupled, two-spin systems and their CFN equivalents are depicted in Table 14.2. The spin echo sequence described is section 14.3 was for an isolated spin; however, the same flow primitive is used in coupled spin systems to represent the evolution of a spin whose chemical shift is refocused and spin partners are decoupled (Table 14.2A). This pulse sequence consists of a 180° pulse on the transverse spin, **I**, placed in the center of the evolution period with no pulse on the coupled partner. As was demonstrated in section 14.3, the spin echo sequence removes all chemical shift evolution leaving only the coupling interaction.

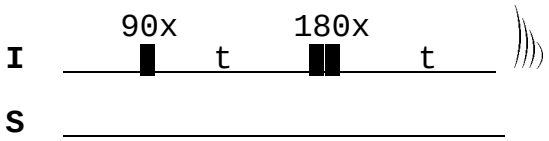

The product operator description is in Equation 14.4.1.

$$\mathbf{I}_x \xrightarrow{\pi/2\hat{\mathbf{I}}_x} -\mathbf{I}_y \xrightarrow{\pi J_{IS} t 2\hat{\mathbf{I}}_z\hat{\mathbf{S}}_z} -\mathbf{I}_y \cos \pi J_{IS} t + 2\mathbf{I}_x\mathbf{S}_z \sin \pi J_{IS} t$$

$$\xrightarrow{\pi\hat{\mathbf{I}}_x} \mathbf{I}_y \cos \pi J_{IS} t + 2\mathbf{I}_x\mathbf{S}_z \sin \pi J_{IS} t$$

$$\xrightarrow{\pi J_{IS} t 2\hat{\mathbf{I}}_z\hat{\mathbf{S}}_z} (\mathbf{I}_y \cos \pi J_{IS} t - 2\mathbf{I}_x\mathbf{S}_z \sin \pi J_{IS} t) \cos \pi J_{IS} t$$

$$+(2\mathbf{I}_x\mathbf{S}_z \cos \pi J_{IS} t + \mathbf{I}_y \sin \pi J_{IS} t) \sin \pi J_{IS} t \qquad (14.4.1)$$

For any value of t the $2\mathbf{I}_x\mathbf{S}_z$ terms cancel leaving Equation 14.4.2:

$$\equiv \mathbf{I}_y (\cos^2 \pi J_{IS} t + \sin^2 \pi J_{IS} t)$$
$$\equiv \mathbf{I}_y \qquad (14.4.2)$$

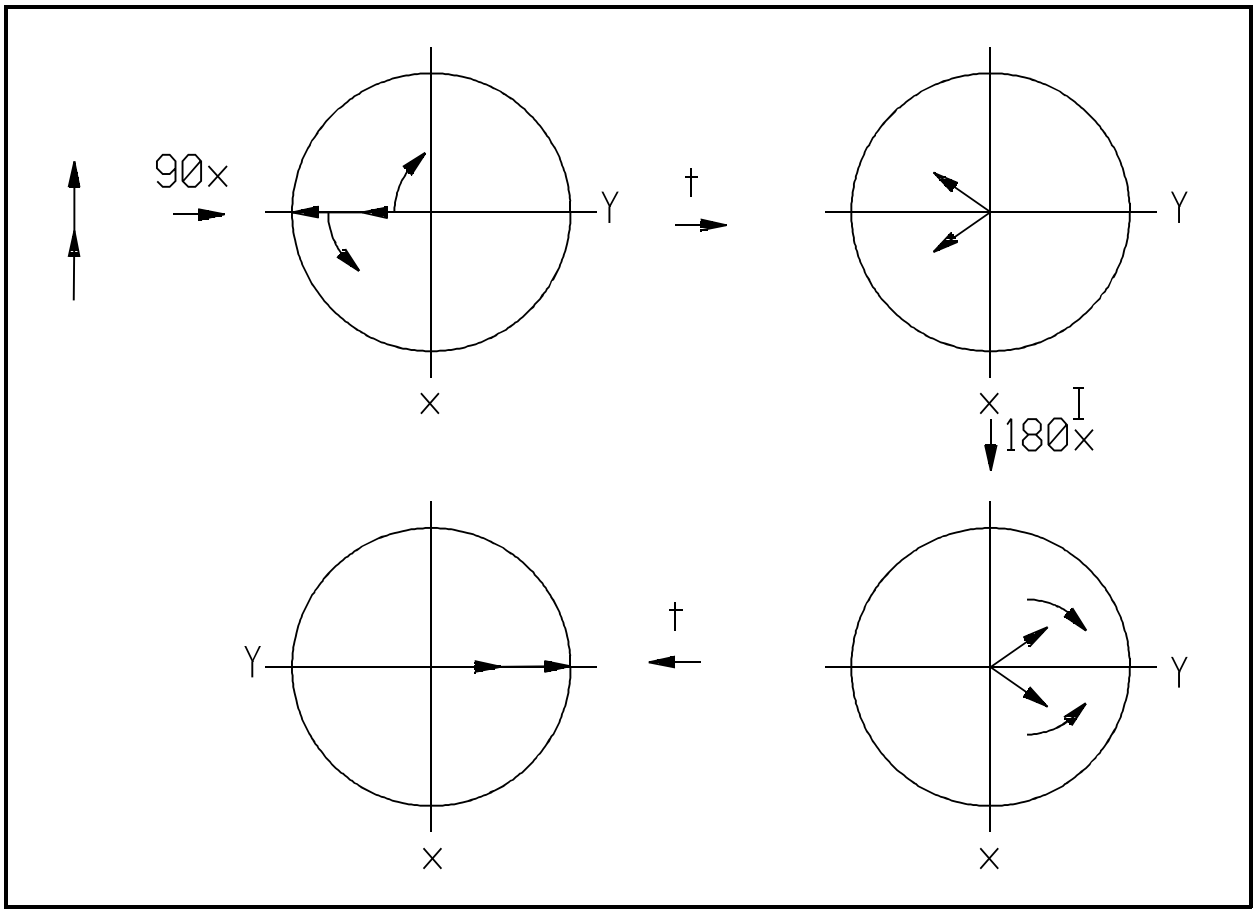

Figure 14.3. Vector picture for **I** selective spin echo sequence in **I-S** coupled spin system.

The rotation operators for this sequence are given in Equation 14.4.3.

$$=\omega_I t\hat{\mathbf{I}}_z=> =\pi J_{IS} t2\hat{\mathbf{I}}_z\hat{\mathbf{S}}_z=> =\pi\hat{\mathbf{I}}_\phi=> =\pi J_{IS} t2\hat{\mathbf{I}}_z\hat{\mathbf{S}}_z=> =\omega_I t\hat{\mathbf{I}}_z=> \quad (14.4.3)$$

The $2\hat{\mathbf{I}}_z\hat{\mathbf{S}}_z$ operator is the weak-scalar-coupling operator. Inserting the identity rotation, $=\pi\hat{\mathbf{I}}_\phi=> =-\pi\hat{\mathbf{I}}_\phi=>$, between the first two operators in Eqn. 14.4.3, one obtains Equation 14.4.4.

$$=\omega_I t\hat{\mathbf{I}}_z=> =\pi\hat{\mathbf{I}}_\phi=> \{=-\pi\hat{\mathbf{I}}_\phi=> =\pi J_{IS} t2\hat{\mathbf{I}}_z\hat{\mathbf{S}}_z=> =\pi\hat{\mathbf{I}}_\phi=>\} =\pi J_{IS} t2\hat{\mathbf{I}}_z\hat{\mathbf{S}}_z=> =\omega_I t\hat{\mathbf{I}}_z=> \quad (14.4.4)$$

The bracketed operators simplify to Equation 14.4.5.

$$=-\pi J_{IS} t2\hat{\mathbf{I}}_z\hat{\mathbf{S}}_z=> \quad (14.4.5)$$

Sequence 14.4.5 combined with the adjacent operator, $=\pi J_{IS}t\mathbf{2}\hat{I}_z\hat{S}_z=>$, in Equation 14.4.3 yields the identity operator as shown in Equation 14.4.6

$$=\omega_I t\hat{I}_z=> =\pi\hat{I}_\phi=> =\hat{I}_E=> =\omega_I t\hat{I}_z=> \quad (14.4.6)$$

Removing the identity operator, we obtain Equation 14.4.7.

$$=\omega_I t\hat{I}_z=> =\pi\hat{I}_\phi=> =\omega_I t\hat{I}_z=> \quad (14.4.7)$$

Placing the same identity operator, $=\pi\hat{I}_\phi=> =-\pi\hat{I}_\phi=>$, at the beginning of sequence 14.4.7, one obtains Equation 14.4.8.

$$=\pi\hat{I}_\phi=> \{ =-\pi\hat{I}_\phi=> =\omega_I t\hat{I}_z=> =\pi\hat{I}_\phi=> \} =\omega_I t\hat{I}_z=> \quad (14.4.8)$$

Reducing the bracketed sequence yields Equation 14.4.9.

$$=\pi\hat{I}_\phi=> =-\omega_I t\hat{I}_z=> =\omega_I t\hat{I}_z=> \quad (14.4.9)$$

Again the adjacent, opposite rotations constitute an identity operator and Equation 14.4.9 simplifies to Equation 14.4.10.

$$=\pi\hat{I}_\phi=> \quad (14.4.10)$$

The evolution of a coupled two-spin system with this pulse sequence is identical to that of an isolated spin (Section 14.3).

14.5. Coupled Two-Spin System - Simultaneous I and S 180° Pulses

For a coupled **I●S** spin system, a spin echo sequence with simultaneous 180° pulses on both nuclei (Table 14.2B), the chemical shift of **I** is suppressed by the mechanism in Section 14.3 but the presence of the 180° pulse on **S** retains the coupling interaction (Figure 14.2).

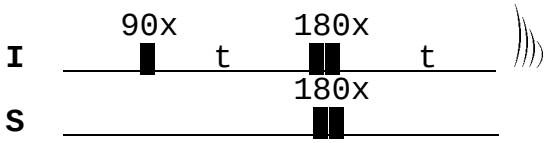

$$\mathbf{I}_x \ =\pi/2\hat{I}_x=> -\mathbf{I}_y \ =\pi J_{IS}\mathbf{t2}\hat{I}_z\hat{S}_z=> -\mathbf{I}_y \cos \pi J_{IS}t + \mathbf{2I_xS_z} \sin \pi J_{IS}t$$

$$=\pi\hat{I}_x=> \mathbf{I}_y \cos \pi J_{IS}t + \mathbf{2I_xS_z} \sin \pi J_{IS}t$$

$$=\pi\hat{S}_x=> \mathbf{I}_y \cos \pi J_{IS}t - \mathbf{2I_xS_z} \sin \pi J_{IS}t$$

$$=\pi J_{IS}t2\hat{I}_z\hat{S}_z => (\mathbf{I}_y \cos \pi J_{IS}t - 2\mathbf{I}_x\mathbf{S}_z \sin \pi J_{IS}t) \cos \pi J_{IS}t$$

$$-(2\mathbf{I}_x\mathbf{S}_z \cos \pi J_{IS}t + \mathbf{I}_y \sin \pi J_{IS}t) \sin \pi J_{IS}t \qquad (14.5.1)$$

If $t = 1/2J_{IS}$ then $\cos \pi/2 = 0$ and $\sin \pi/2 = 1$ and Equation 14.5.2 is obtained.

$$\equiv -\mathbf{I}_y \qquad (14.5.2)$$

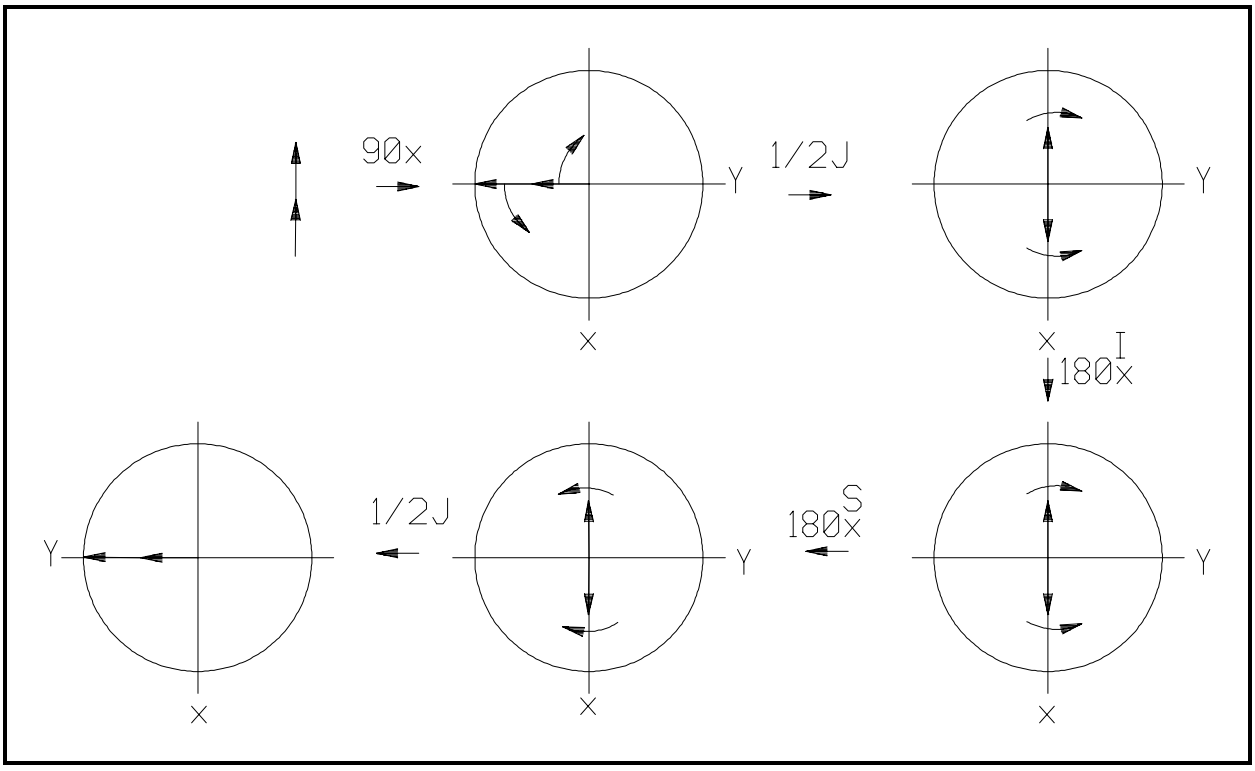

Figure 14.4. Vector picture for spin echo sqeuence of **I-S** spin system with 180° pulses on both spins.

The appropriate rotation operators are given in Equation 14.5.3.

$$=\omega_I t\hat{I}_z => =\pi J_{IS}t2\hat{I}_z\hat{S}_z => =\pi(\hat{I}_\phi+\hat{S}_{\phi'}) => =\pi J_{IS}t2\hat{I}_z\hat{S}_z => =\omega_I t\hat{I}_z => \qquad (14.5.3)$$

The resulting composite rotation consists of three simple rotations (Equation 14.5.4).

$$=\pi\hat{S}_{\phi'} => =\pi\hat{I}_\phi => =\pi J_{IS}2t2\hat{I}_z\hat{S}_z => \qquad (14.5.4)$$

The 180° pulse on the **S** spin can be eliminated since it does not affect the detected **I** spin, giving Equation 14.5.5.

$=\pi\hat{\mathbf{I}}_{\phi}=>\ =\pi J_{IS}2t\mathbf{2}\hat{\mathbf{I}}_z\hat{\mathbf{S}}_z=>$ (14.5.5)

In addition to the phase shift arising from the 180°_{ϕ} pulse, there is an evolution due to the active coupling interaction. The CFN descriptor for this evolution (Table 14.2B) is a flow primitive **E** that is combined with an active coupling modifier **A** connecting the spin tier of the transverse spin, **I**, with that of its coupling partner, **S**. Active coupling causes the evolution of inphase coherence into an antiphase state (or *vice-versa*) between the coupled spins. For a spin with more than one coupling partner, multiple coupling modifiers connect the evolving coherence with the respective spin tiers.

14.6. Coupled Two-Spin System - Selective S 180° pulse

The two other sequences (Table 14.2C and 14.2D) do not have a 180° pulse on the transverse component **I** and thus there is chemical shift evolution. The sequence in Table 14.2C represents a spin evolving under the chemical shift operator, Table 14.1**CS**, while the coupling interaction to **S** is refocused (decoupled) by the application of a 180° pulse to **S**. For a coupled **I●S** spin system with **S** selective 180° pulse ($=\pi\hat{\mathbf{S}}_x=>$). The chemical shift of **I** is not suppressed in general, but can be set to zero by putting the **I** spin on resonance, *i. e.* the effective frequency ω_I is 0. This little bit of cheating does not damage the credibility of the analysis. Figure 14.4 diagrams the behavior of this pulse sequence in the presence of chemical shift.

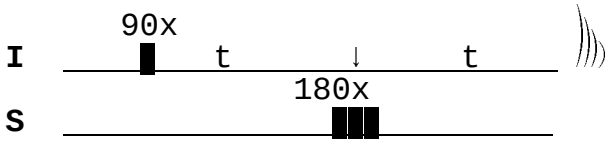

The product operator analysis for this sequence is given in Equation 14.6.1.

$$\mathbf{I}_x\ =\pi/2\hat{\mathbf{I}}_x=>\ -\mathbf{I}_y\ =\pi J_{IS}\mathbf{t}\mathbf{2}\hat{\mathbf{I}}_z\hat{\mathbf{S}}_z=>\ -\mathbf{I}_y\cos\pi J_{IS}t+\mathbf{2I}_x\mathbf{S}_z\sin\pi J_{IS}t$$

$$=\pi\hat{\mathbf{S}}_x=>\ -\mathbf{I}_y\cos\pi J_{IS}t-\mathbf{2I}_x\mathbf{S}_z\sin\pi J_{IS}t$$

$$=\pi J_{IS}\mathbf{t}\mathbf{2}\hat{\mathbf{I}}_z\hat{\mathbf{S}}_z=>\ -(\mathbf{I}_y\cos\pi J_{IS}t\ -\mathbf{2I}_x\mathbf{S}_z\sin\pi J_{IS}t)\cos\pi J_{IS}t$$

$$-(\mathbf{2I}_x\mathbf{S}_z\cos\pi J_{IS}t+\mathbf{I}_y\sin\pi J_{IS}t)\sin\pi J_{IS}t \qquad (14.6.1)$$

Again, for any value of t the $\mathbf{2I}_x\mathbf{S}_z$ terms cancel leaving Equation 14.6.2.

$$\equiv -\mathbf{I}_y(\cos^2\pi J_{IS}t+\sin^2\pi J_{IS}t)$$

$$\equiv -\mathbf{I}_y \qquad (14.6.2)$$

The rotations for this sequence are given in Equation 14.6.3.

$$=\omega_I t\hat{I}_z=> \;=\pi J_{IS} t 2\hat{I}_z\hat{S}_z=> =\pi\hat{S}_\phi=> \;=\pi J_{IS} t 2\hat{I}_z\hat{S}_z=> =\omega_I t\hat{I}_z=> \qquad (14.6.3)$$

After the insertion of the appropriate identities, the composite rotation arising from this sequence is given in Equation 14.6.4.

$$=\omega_I 2t\hat{I}_z=> \qquad (14.6.4)$$

which is the same as for the chemical shift evolution of an isolated spin.

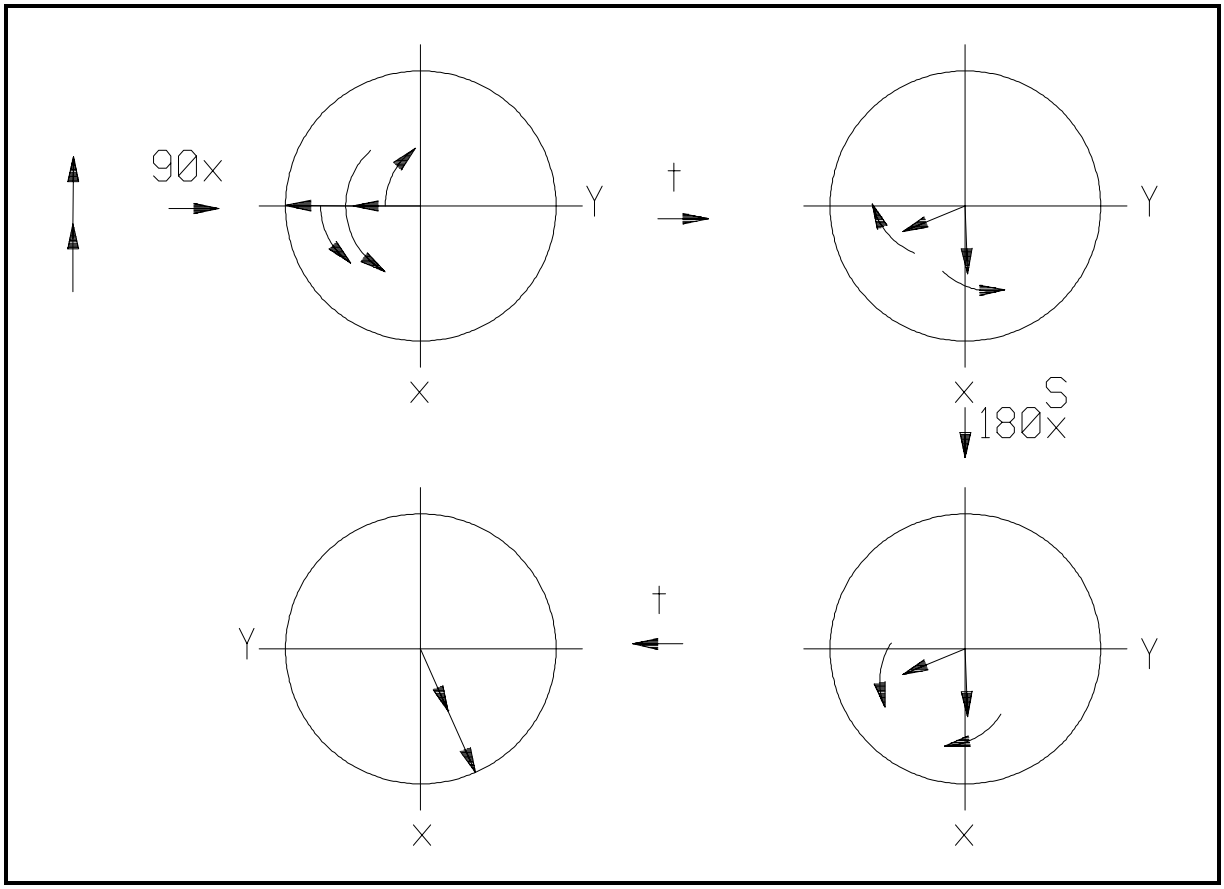

Figure 14.5. Vector picture for a spin **I** precessing under chemical shift and coupling to another spin **S**. The coupling interaction is refocused by the 180° pulse applied to the **S** spin in the center of the sequence.

The rotations for this sequence are in Equation 14.6.5.

$$=\omega_I t\hat{I}_z=> \;=\pi J_{IS} t 2\hat{I}_z\hat{S}_z=> =\pi\hat{S}_\phi=> \;=\pi J_{IS} t 2\hat{I}_z\hat{S}_z=> =\omega_I t\hat{I}_z=> \qquad (14.6.5)$$

After the insertion of the appropriate identities, the composite rotation arising from this sequence is given in Equation 14.6.6.

$$=\omega_I 2t\hat{\mathbf{I}}_z=> \qquad (14.6.6)$$

This is the same rotation obtained for the chemical shift evolution of an isolated spin. Above, where we assumed that $\omega_I=0$, there would be an overall identity rotation. Notice that if there is a 180° pulse applied to either spin of the coupled pair of spins, the coupling interaction is eliminated.

14.7. Coupled Two-Spin System - No 180° pulses

Table 14.2D represents a spin evolving under the chemical shift operator, Table 1.1**CS**, with active coupling, Table 1.1**A**, to another spin. After the initial 90° pulse, there are no pulses applied to the spins and the transverse **I** spin evolves under both chemical shift and coupling. Equation 14.7.1 is the series of rotations for this sequence.

$$=\omega_I t\hat{\mathbf{I}}_z=> \;=\pi J_{IS} t 2\hat{\mathbf{I}}_z\hat{\mathbf{S}}_z=> \qquad (14.7.1)$$

Both chemical shift and coupling are active during this sequence. No simple composite rotation is available for this sequence.

The use of the CFN description gives a visualization of the mechanism involved in multipulsed, multinuclear experiments. By introducing a graphical nomenclature, complicated experiments can be explained simply. In the remainder of this course, the CFN diagrams will be used as an aid in the description of two dimensional experiments. The utility of this description becomes even more apparent for three- and higher-dimensional experiments, in which evolutions on different nuclei occur simultaneously and the number of pulses and delays in the sequence is large.

1. R. Benn and H. Günther (1983) *Angew. Chem. Int. Ed. Engl.* **22**, 350.

2. C. J. Turner (1984) *Prog. NMR Spectrosc.* **16**, 311.

3. O. W. Sørensen, G. W. Eich. M.H. Levitt, G. Bodenhausen, and R. R. Ernst (1983) *Prog. NMR Spectrosc.* **16**, 163.

4. F. J. M. van de Ven and C. W. Hilbers (1983) *J. Magn. Reson.* **54**, 512.

5. K. J. Packer and K. M. Wright (1983) *Mol. Phys.* **50**, 797.

6. U. Eggenberger and G. Bodenhausen (1990) *Angew. Chem. Int. Ed. Engl.* **29**, 374.

7. M. Ikura, L. E. Kay, and A. Bax (1990) *J. Magn. Reson.* **29**, 496.

8. G. M. Clore and A. M. Gronenborn (1991) *Prog. NMR Spectrosc.* **23**, 43.